The FEBS Journal

FEBS PRESS science publishing by scientists

DNA-damage inducible protein 1 is a conserved metacaspase substrate that is cleaved and further destabilized in yeast under specific metabolic conditions

León A. Bouvier†, Gabriela T. Niemirowicz†, Emir Salas-Sarduy, Juan José Cazzulo and Vanina E. Alvarez

Instituto de Investigaciones Biotecnológicas - Instituto Tecnológico de Chascomús (IIB-INTECH), Universidad Nacional de San Martín (UNSAM) - Consejo Nacional de Investigaciones Científicas y Técnicas (CONICET), Buenos Aires, Argentina

Keywords
calcium; Ddi1; metacaspase; substrate; UBA

Correspondence
V. E. Alvarez, Instituto de Investigaciones Biotecnológicas - Instituto Tecnológico de Chascomús (IIB-INTECH), Universidad Nacional de San Martín (UNSAM) - Consejo Nacional de Investigaciones Científicas y Técnicas (CONICET). Campus Miguelete, Av. 25 de Mayo y Francia, 1650 San Martín, Buenos Aires, Argentina
Fax: +54 11 4006-1559
Tel: +54 11 4006-1500 ext 2121
E-mail: vanina.eder.alvarez@gmail.com

†These authors contributed equally to this work

(Received 17 July 2017, revised 29 November 2017, accepted 17 January 2018)

doi:10.1111/febs.14390

Metacaspases, distant relatives of metazoan caspases, have been shown to participate in programmed cell death in plants and in progression of the cell cycle and removal of protein aggregates in unicellular eukaryotes. However, since natural proteolytic substrates have scarcely been identified to date, their roles in these processes remain unclear. Here, we report that the DNA-damage inducible protein 1 (Ddi1) represents a conserved protein substrate for metacaspases belonging to divergent unicellular eukaryotes (trypanosomes and yeasts). We show that although the recognized cleavage sequence is not identical among the different model organisms tested, in all of them the proteolysis consequence is the removal of the ubiquitin-associated domain (UBA) present in the protein. We also demonstrate that Ddi1 cleavage is tightly regulated *in vivo* as it only takes place in yeast when calcium increases but under specific metabolic conditions. Finally, we show that metacaspase-mediated Ddi1 cleavage reduces the stability of this protein which can certainly impact on the many functions ascribed for it, including shuttle to the proteasome, cell cycle control, late secretory pathway regulation, among others.

Introduction

Metacaspases, together with paracaspases, were originally identified as distant relatives of canonical caspases based on sequence homology and predicted secondary structure [1]. While paracaspases can be found alongside caspases in metazoan organisms modulating NF-κB pathway [2], metacaspases are only present in plants, fungi, and protozoa. Metacaspases can be divided into different types according to their domain composition. The type I metacaspases could have (or not) amino terminal protein-protein interaction domains such as proline rich regions or a zinc finger motif and invariantly have a metacaspase C-terminal domain. Type II metacaspases do not possess this kind of prodomains but contain a long linker between the p20 and p10 homologous regions and are only found in plants [3].

Despite their initial classification into clan CD family C14, the biochemical characterization of

Abbreviations
Abz, ortho-aminobenzoyl; Ddi1, DNA-damage inducible protein 1; Dnp, N-(2,4-dinitrophenyl)-ethylenediamine; DTT, dithiothreitol; GST, Glutathione S-transferase; HA, hemagglutinin; HEPES, N-[2-hydroxyethyl] piperazine-N′-[2-ethanesulfonic acid]; IAM, iodoacetamide; RVP, retroviral protease-like domain; TBS, tris-buffered saline; UBA, ubiquitin-associated domain; UbL, ubiquitin-like domain.

metacaspases showed a number of singularities. Some of these differences are now apparent when analyzing the three dimensional structure of metacaspases from *Trypanosoma brucei* (*Tb*MCA2) and *Saccharomyces cerevisiae* (Yca1p) [4,5]. These enzymes exhibit an overall fold similar to caspases but with two extra beta strands preventing their dimerization. In addition, a large acidic pocket explains the contrasting substrate specificity for basic amino acid residues. In *Tb*MCA2, an unusual N-terminus sterically occludes the active site and calcium binding, mediated by four conserved aspartic acid residues, might lead to a conformational change that switches the catalytic dyad to a competent state [4].

Regardless of their significantly different biochemical properties, metacaspases have been shown to mediate cell death during stress responses and development in plants [6–9]. In unicellular organisms, nondeath roles were proposed for metacaspases. In yeast, Yca1p deletion or inactivation results in a prolonged G1/S transition and a defective G2/M checkpoint, suggesting that this protein might regulate cell cycle dynamics [10]. In kinetoplastids, the phenotypes observed in RNAi studies in *T. brucei* [11] or overexpression experiments in the case of *L. major* [12] and *T. cruzi* [13] also suggest that metacaspases might control cell cycle progression.

Beneficial rather than deleterious effects were recognized lately to metacaspases when protein homeostasis was impaired. Yca1p assists to degrade misfolded proteins that accumulate during aging or that are generated by acute stress. In this case, both scaffolding functions of the protein as well as intrinsic peptidase activity, were demonstrated to be important for lifespan control [14]. However, the cleavage events supporting these proposed roles are largely unknown.

So far, a limited number of substrates has been discovered. For *Picea abies* metacaspase, one common target with caspase-3 was described, and this finding was used to argument for the existence of an evolutionary conserved programmed cell death pathway in plants [15]. In addition, the glycolytic enzyme glyceraldehyde-3-phosphate dehydrogenase [16] and the poly(ADP-ribose) polymerase were reported as fungi metacaspase substrates [17]. Although the cleavage of both enzymes was related to programmed cell death, the relevance and consequences of these proteolytic events remain unclear. More recently, proteome-wide substrate searches were performed by means of comparative proteomic methodologies for metacaspase-9 of *Arabidopsis thaliana* and metacaspase of *Candida albicans*. The potential substrates identified in these studies suggest roles of the plant metacaspase in processes other than those related to cell death [18] and involve the yeast protease in protein folding, protein aggregate resolubilization, glycolysis, mitochondrial functions, [19] and protein glycosylation [20].

In this work, we have identified the DNA-damage inducible protein 1 (Ddi1) as a natural metacaspase substrate. Ddi1 belongs to a group of shuttle proteins that deliver polyubiquitinated cargoes for degradation due to their ability to interact with the proteasome through their ubiquitin-like (UbL) domain and at the same time with ubiquitinated substrates through their ubiquitin associated domain(s) (UBA) [21]. Here, we show that metacaspase-mediated cleavage of Ddi1 is conserved among very divergent unicellular eukaryotes and that, although the recognized cleavage sequence is not identical among the different model organisms tested, in all of them the proteolysis consequence is the removal of the UBA domain. We demonstrate that Ddi1 cleavage is tightly regulated *in vivo* as it only takes place in yeast when calcium increases but under specific metabolic conditions. Finally, we show that Ddi1 cleavage reduces the stability of the protein potentially affecting many diverse and important cellular processes.

Results

Identification of an *in vitro* protein substrate among metacaspase interactors

To gain insights on how the different metacaspase isoforms present in *T. cruzi* (*Tc*MCA3 and *Tc*MCA5) participate in the biology of the parasite, we sought to establish their specific set of interacting proteins. Immunoaffinity purification of 3xFLAG-tagged metacaspases expressed in transgenic epimastigote cell lines [13] followed by Liquid Chromatography-Mass Spectrometry (LC-MS/MS) analysis, led to the identification of a number of putative partners (Table S1). To study these interactions *in vitro*, a bacterial co-expression system was devised. Putative interactors were expressed in *E. coli* as C-terminally GST fusion proteins along with active or inactive 3xFLAG-tagged metacaspase variants (Fig. 1). Thus, the interactions could be evaluated through glutathione affinity purification followed by western blot analysis of GST and 3xFLAG tags.

For one of the assayed candidates, the DNA damage inducible protein 1 (*Tc*DDI1), coexpression with *Tc*MCA5 produced an additional protein fragment not present when the protease was replaced with the C201A inactive mutant (Fig. 2A, 0 h). In cleared

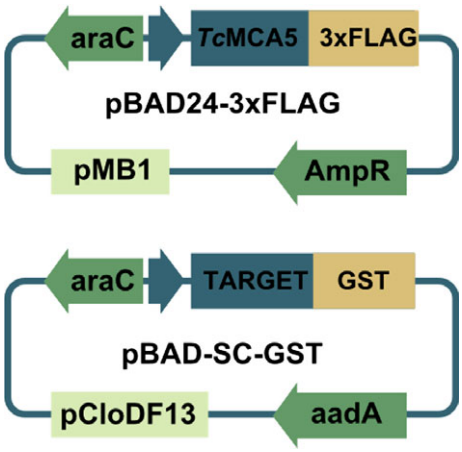

Fig. 1. *In vitro* coexpression system. Schematic representation of the plasmids used to co-express *Tc*MCA5 with its interacting proteins. pBAD24 carrying the PMB1 replicon and the ampicillin resistance gene (AmpR) was designed to direct the expression of C-terminal 3xFLAG-tagged *Tc*MCA5. pBAD-SC-GST carries the CloDF13 replicon, the streptomycin/spectinomycin resistance gene (aadA) and drives the co-expression of individual interacting proteins as N-terminal fusions to glutathione S-transferase (GST). See Table S2 for additional plasmid information.

lysates supplemented with calcium, a reported enhancer of metacaspase activity, the abundance of this fragment increased in a time dependent manner (Fig. 2A, 5 h, 16 h). Indeed, N-terminal sequencing of the fragment showed that the cleavage took place after the arginine 377 residue in the QQR-GS sequence (not shown), in agreement with the reported specificity for basic amino acids of these proteases.

Since Ddi1 is a particular shuttle protein that bears, in addition to the UbL and UBA domains, a central retroviral protease-like domain (RVP) we evaluated the expression profile of an equivalent D248A inactive mutant and conclude that none of the fragments is produced as a consequence of autoproteolytic activity (Fig. 2B). Moreover, to verify that *Tc*DDI1 was indeed being cleaved by *Tc*MCA5, ruling out any downstream activated bacterial protease, we performed *in vitro* proteolysis assays with purified recombinant proteins. Fragment patterns of *Tc*DDI1-GST were comparable to those obtained by incubation with *Tc*MCA5 in the presence of the general cysteine peptidase inhibitor iodoacetamide (IAM) (Fig. 3, left panel). However, when the inhibitor was removed from the reaction mix, the proteolytic processing took place. The position and specificity of the cleavage was confirmed to be at R377, since mutation of this residue into alanine completely abolished metacaspase mediated processing (Fig. 3, right panel).

Ddi1 is a conserved metacaspase substrate *in vitro*

To assess if Ddi1 could also be substrate for other metacaspases, the study was extended to include the orthologous substrate/peptidase pairs from *T. brucei*, another kinetoplastid parasite, and that from the more distant organism *S. cerevisiae*. Each respective gene was cloned, expressed in *E. coli* as a GST-fusion and the resulting purified recombinant proteins were used for *in vitro* cleavage assays.

As shown in Fig. 4, *Tb*MCA5 processed *Tb*DDI1 close to the C-terminus. According to N-terminal sequencing of the resulting C-terminal fragments, cleavage took place after R292 and R325. Disruption of the first site by R292A mutation increased proteolysis at R325. On the other hand, replacing the 325 arginine residue by alanine in the second site, not only enhanced proteolysis after R292, but also gave rise to an additional cleavage site, offset by one residue toward the N-terminus, at K324 (labeled with an asterisk in Fig. 4A, left panel). Cleavage at this third site resulted more evident in the R292A/R325A (double mutant) and was completely abolished in the R292A/K324A/R325A (triple mutant) (Fig. 4A, right panel).

Similarly, yeast metacaspase Yca1p is able to process Ddi1p at more than one position, namely after R367 and R377. The cleavage sites were determined by Edman degradation of the processed fragments and subsequently validated by individual or simultaneous alanine substitutions of the arginine residues (Fig. 4B). Note that an additional ~ 39 kDa fragment, not detectable in the sample corresponding to the WT substrate, becomes apparent in derivatives when the preferred cleavage sites are mutated.

For the three substrate/peptidase pairs analyzed, *Tb*MCA5 turned out to be the most efficient, reaching a k_{cat}/K_M value of 1.9×10^4 $M^{-1} \cdot s^{-1}$. The catalytic efficiency for *Tc*MCA5 and Yca1p on their respective substrates was estimated at 3.5×10^3 $M^{-1} \cdot s^{-1}$ and 2.0×10^3 $M^{-1} \cdot s^{-1}$ (Fig. 5).

Metacaspase exscinds the UBA domain from Ddi1 proteins

Ddi1 displays a characteristic modular architecture (Fig. 6A). Remarkably, all Ddi1 proteins were cleaved at the RVP-UBA domain boundaries, even when the protein sequence identity along this region is considerably low. Alignment of the Ddi1 sequences in the vicinity of the cleavage sites (Fig. 6B) suggests that besides the well-known strict specificity for basic amino acid residues at the P1 position, metacaspases

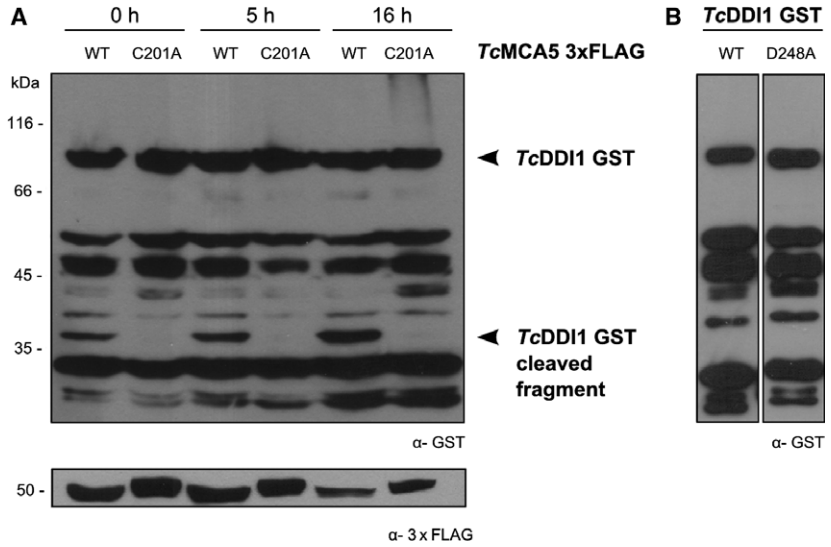

Fig. 2. *Tc*DDI1 cleavage in bacteria co-expressing *Tc*MCA5. (A) Time course studies of *Tc*DDI1 cleavage by *Tc*MCA5 in *E. coli* BL21(DE3) harboring plasmids pBAD-SC-*Tc*DDI1-GST and pBAD24-*Tc*MCA5-3xFLAG (WT) or the corresponding metacaspase active site mutant (C201A). Cells were grown at 37 °C up to $OD_{600} \approx 0.6$, induced with 0.2% arabinose for 3 h, and disrupted in lysis buffer supplemented with 100 μM $CaCl_2$ and 10 mM DTT to stimulate metacaspase activity. Samples were taken at the indicated time points and subjected to western blotting with anti-GST antibodies (Top panel). Full length and C-terminal proteolysis fragment are marked with arrowheads. *Tc*MCA5 presence in all samples was confirmed using anti-FLAG antibodies (Bottom panel). (B) Immunoblot analysis of recombinant wild-type and active site mutant (D248A) *Tc*DDI1 purified by glutathione-affinity chromatography. For both constructs, overexpression resulted in the production of the full length protein together with additional fragments, which most likely correspond to bacterial degradation products.

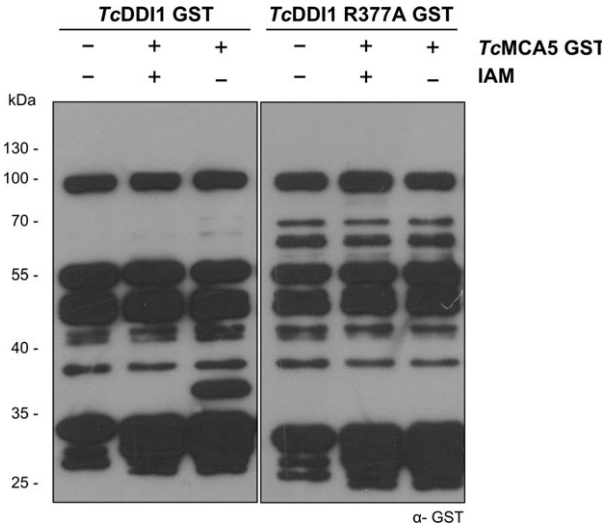

Fig. 3. *In vitro* processing of *Tc*DDI1 by *Tc*MCA5 using purified recombinant proteins. Purified recombinant *Tc*DDI1-GST (25 μg) was incubated with *Tc*MCA5-GST (2.5 μg) in 200 μL of 50 mM HEPES pH 7.2 containing 100 μM $CaCl_2$, 10 mM DTT and 10% glycerol in the presence (+) or absence (–) of 20 mM iodoacetamide (IAM). After 1 h at 37 °C, 20 μL samples were separated in 12.5% SDS/PAGE, transferred to nitrocellulose membranes and analyzed by western blot using anti-GST monoclonal antibodies. Similar reactions were performed for the R376A cleavage site mutant.

might prefer polar groups (S, T) or small (G) residues at the first and second positions C-terminal to the site of cleavage (P1′ and P2′ respectively).

Based on these sequences we designed five FRET substrates with the general form Abz-XXXRXXXK (Dnp) to evaluate if metacaspase cleavage can also take place in the context of a short peptide. When initial rates for the enzymatic hydrolysis were determined using identical stocks of enzymes and substrates, we found that all but one of the tested substrates were cleaved. For each enzyme the highest catalytic efficiency was obtained with Abz-AAKRSTAK(Dnp) as substrate (Table 1). Noteworthy, this novel peptide is cleaved by the *T. cruzi* and yeast metacaspases more efficiently than the model substrate Z-VRPR-AMC. Interestingly, the peptide Abz-PTGRSTAK(Dnp), which shares identical P1-P4′ positions with the most efficient substrate, was resistant to metacaspase cleavage.

Yeast Ddi1p is cleaved by Yca1p *in vivo*

To assess if Ddi1p could undergo metacaspase mediated proteolytic processing in yeast, the *DDI1* gene was endogenously N-terminal HA-tagged in strains with wild-type *YCA1* as well as null *yca1Δ* and

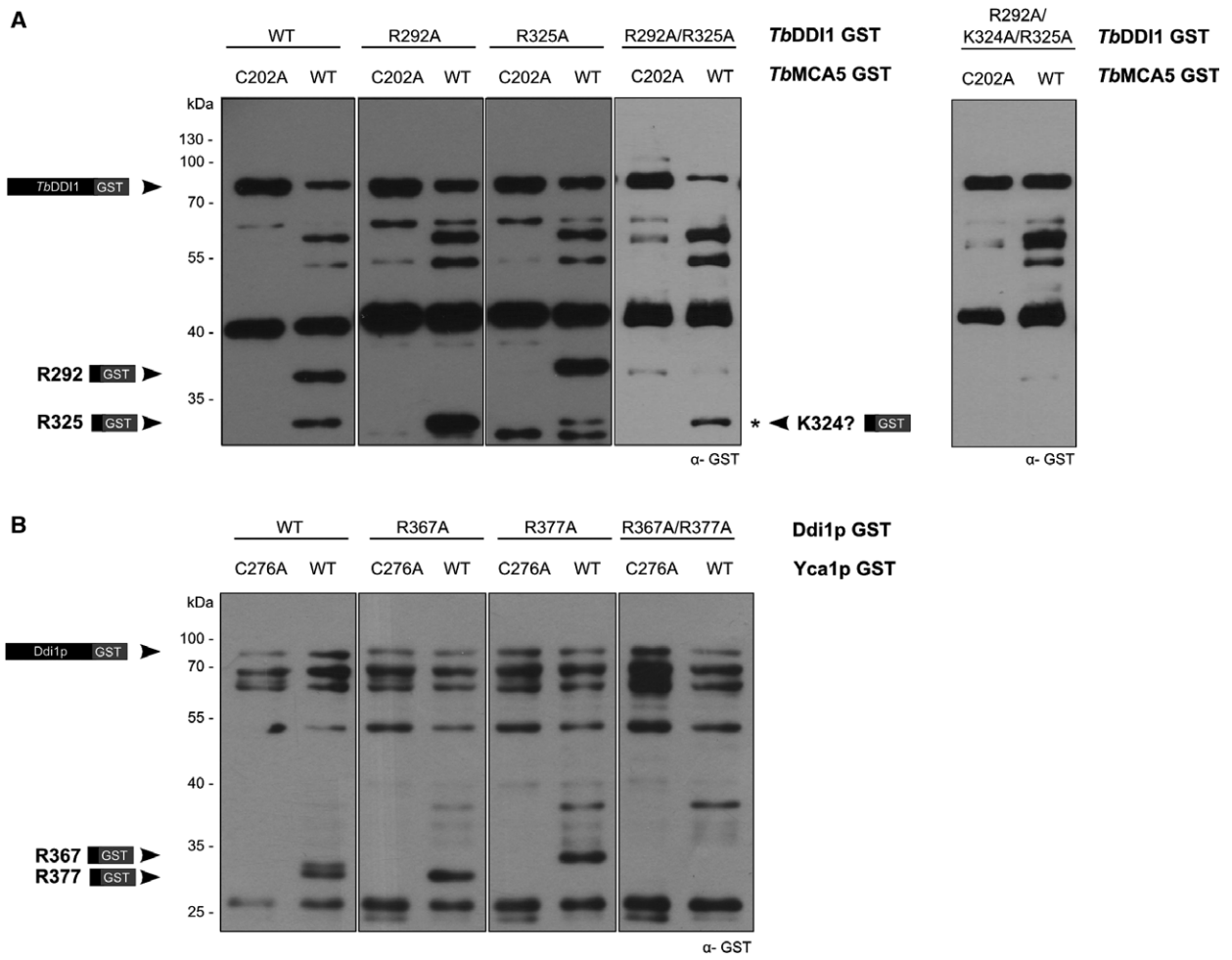

Fig. 4. Ddi1 is a conserved metacaspase substrate. (A) *In vitro* cleavage reactions for *Tb*DDI1-GST using *Tb*MCA5 (WT) or the corresponding active site mutant (C202A). Single and double mutants at the cleavage sites identified by Edman degradation (R292A and R325A) were analyzed by western blot using anti-GST antibodies. A triple mutant (R292A, K324A, R3245) including a third potential cleavage site (whose proteolysis fragment is labeled with an asterisk) was evaluated similarly. Relevant protein species are marked with arrowheads and depicted to the left. (B) *In vitro* cleavage reactions for Ddi1p-GST and individual or combined double mutants (R367A and R377A) using Yca1p (WT) or the corresponding active site mutant (C276A). All reactions were carried out using 25 μg of each tested substrate and 2.5 μg of the corresponding peptidase in 200 μL of 50 mM HEPES pH 7.2 containing 100 μM $CaCl_2$, 10 mM DTT, and 10% glycerol.

inactive $yca1^{C276A}$ mutant backgrounds. Western blot analysis showed that in all three transgenic strains Ddi1p is mainly present in both its phosphorylated and unphosphorylated forms [22] but without any differential cleavage product among them (not shown).

Since structural studies have shown that calcium stabilizes metacaspase active site we examined if an increase in the cytosolic levels of this cation caused by ionophores or environmental stimuli (such as the addition of glucose to nutrient-starved cells (G-TECC) [23,24]) could eventually lead to Ddi1p processing. The use of calcium ionophores A23187 or ionomycin did not alter Ddi1p pattern in the different metacaspase backgrounds (Fig. 7A). However, when calcium influx was mediated by addition of glucose (Fig. 7B) an additional pair of bands could be detected in the sample relative to the *YCA1* strain (Fig. 7A). The molecular weight of these fragments (~43 kDa) as well as the fact that they remained undetectable in the samples derived from the strains lacking an active metacaspase ($yca1^{C276A}$) suggested that they could be the result of Yca1p mediated *in vivo* cleavage of the HA-Ddi1p fusion protein at R367 and R377. To verify this possibility the HA-*DDI1* gene in the *YCA1* background was replaced by equivalents that code for the previously identified single and double, arginine to alanine,

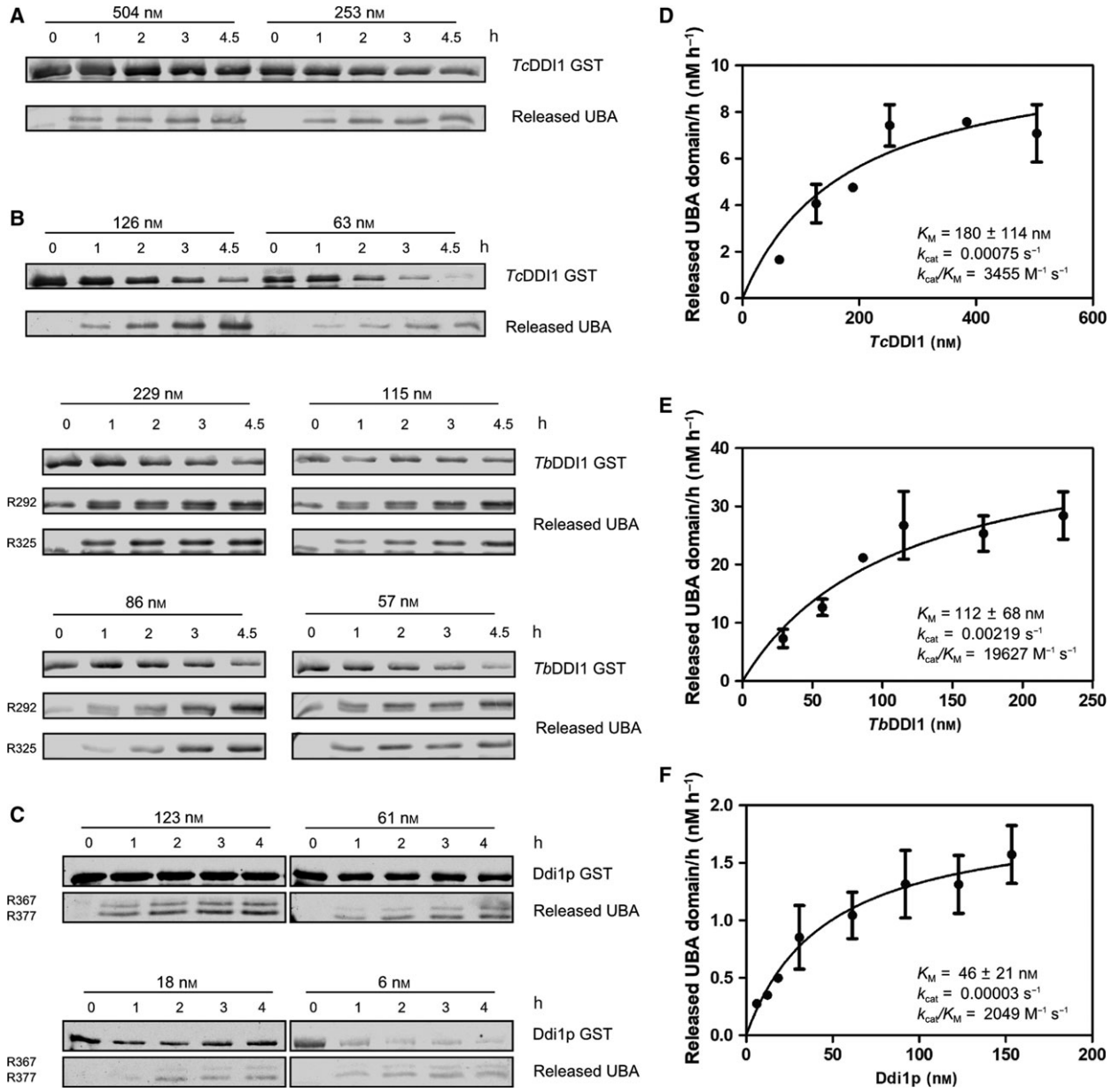

Fig. 5. Kinetic analysis for Ddi1 processing reactions. (A–C) western blot analysis of time-course processing reactions of Ddi1 proteins at different concentrations (four of them are shown on top of the Westerns). The assays were performed at 37 °C in 50 mM HEPES pH 7.2 containing 100 μM $CaCl_2$, 10 mM DTT and 10% glycerol. Reactions were stopped at indicated times by mixing with Laemmli sample buffer and subsequently assessed by 12.5% SDS/PAGE, followed by western blot using anti-GST monoclonal antibodies. Bands were detected using an Odyssey laser-scanning system and quantified with Image Studio software. The fluorescent signal of full length Ddi1 proteins and cleaved products were used to determine the processing rates as described in [46]. (D–F) Michaelis-Menten graphical analysis of metacaspases processing rates with Ddi1 proteins. Data were obtained at least in duplicate to determine standard deviations. The error of the K_M value represents the standard error on the fit.

metacaspase cleavage resistant mutants. As shown in Fig. 8, while *in vivo* Ddi1p cleavage was prevented at each corresponding site in the single R367A and R377A mutants, it was completely blocked in the double R367A/R377A.

Removal of the C-terminal UBA domain can reduce the stability of Ddi1p

To assess the effects of Yca1p mediated proteolytic processing, we compared the expression profiles of

endogenously HA-tagged full length Ddi1p to those of derived mutants that mimic the possible products of metacaspase cleavage (HA-Ddi1p$^{1\text{-}367}$ and HA-Ddi1p$^{1\text{-}377}$). Both shorter variants showed a four-fold reduction in their respective steady-state abundances (Fig. 9A). To establish if such reduction could be a consequence of lowered protein stability, cycloheximide chase assays were performed. While the half-life of α-tubulin in all three genetic backgrounds remained constant (> 20 h) that of the different Ddi1p variants decreased from > 15 h, for the full length fusion protein, to 2 h for HA-Ddi1p$^{1\text{-}367}$ and HA-Ddi1p$^{1\text{-}377}$ (Fig. 9B).

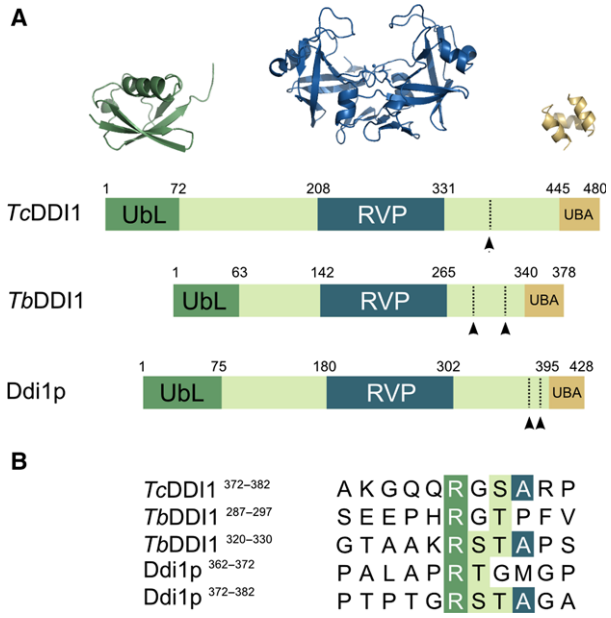

Fig. 6. Metacaspase exscinds the UBA domain from Ddi1 proteins. (A) The cleavage sites identified by Edman degradation (marked with arrowheads) were located between the retroviral protease-like domain (RVP) of Ddi1 proteins and the ubiquitin-associated domains (UBA), responsible for interacting with ubiquitylated cargos. (B) Alignment of the Ddi1 sequences in the vicinity of the cleavage sites.

Altogether our results suggest that metacaspase might directly interfere with Ddi1 functions through proteolytic removal of the UBA domain or indirectly by destabilizing the full length protein.

Discussion

In this study, we describe how Ddi1 protein is cleaved by metacaspases in different model organisms: *T. cruzi*, *T. brucei,* and *S. cerevisiae*. For the three metacaspase/Ddi1 protein pairs analyzed, processing sites were located between the RVP and UBA domains. Despite the low sequence identity shared in this region (11%–21% according to pairwise alignments), N-terminal sequencing experiments revealed, in addition to the stringent specificity for basic amino acids at P1 position, a marked preference for polar and/or small amino acids at P1′and P2′. Other identified type I metacaspase cleavage sites in protein substrates (Table 2) also support the specificity for small side chain amino acids after the scissile bond. This feature, shared with caspases and paracaspases [2], contrasts the preferred acidic residue at P1′ reported for the type II metacaspase 9 of *A. thaliana* [18]. Regarding the catalytic efficiency of these enzymes, the values obtained for metacaspases on Ddi1 proteins are comparable to those reported for the human paracaspase MALT1 on its protein substrate CYLD (10^3–10^4 $M^{-1}\cdot s^{-1}$) [25].

The use of peptide substrates derived from the cleavage sites in the Ddi1 orthologues hinted at the high selectivity of metacaspases. Whereas the Abz-AAKR-STAK(Dnp) FRET substrate was hydrolyzed with the highest k_{cat}/K_M values by all three metacaspases used, Abz-PTGRSTAK(Dnp) remained intact even though both peptides share identical residues spanning P1 to P4′. The presence of a Lys residue at P2 in the former might explain these differences since it matches the reported preference of *Tb*MCA2 when acting on small peptide substrates [26]. Furthermore, the fact that the site in Ddi1p corresponding to the noncleavable FRET

Table 1. Comparative catalytic efficiencies of *Tc*MCA5, *Tb*MCA5 and Yca1p on FRET substrates. Values for the enzyme concentration were obtained using active-site-titrated enzymes, as described in the experimental section. R, Resistant; n.d., not detected.

Substrate	*Tc*MCA5 k_{cat}/K_M ($M^{-1}\cdot s^{-1}$)	*Tb*MCA5 k_{cat}/K_M ($M^{-1}\cdot s^{-1}$)	Yca1p k_{cat}/K_M ($M^{-1}\cdot s^{-1}$)
Abz-GQQRGSAK(Dnp)	3.64 ± 0.13	81.31 ± 3.00	294.15 ± 15.93
Abz-AAKRSTAK(Dnp)	9.09 ± 0.36	123.9 ± 6.67	3446.24 ± 82.78
Abz-EPHRGTPK(Dnp)	n.d.	32.61 ± 0.68	63.43 ± 2.99
Abz-LAPRTGMK(Dnp)	6.78 ± 0.41	37.95 ± 0.76	1510.39 ± 93.92
Abz-PTGRSTAK(Dnp)	R	R	R
Z-VRPR-AMC	2.82 ± 0.09	459.55 ± 10.04	581.03 ± 9.53

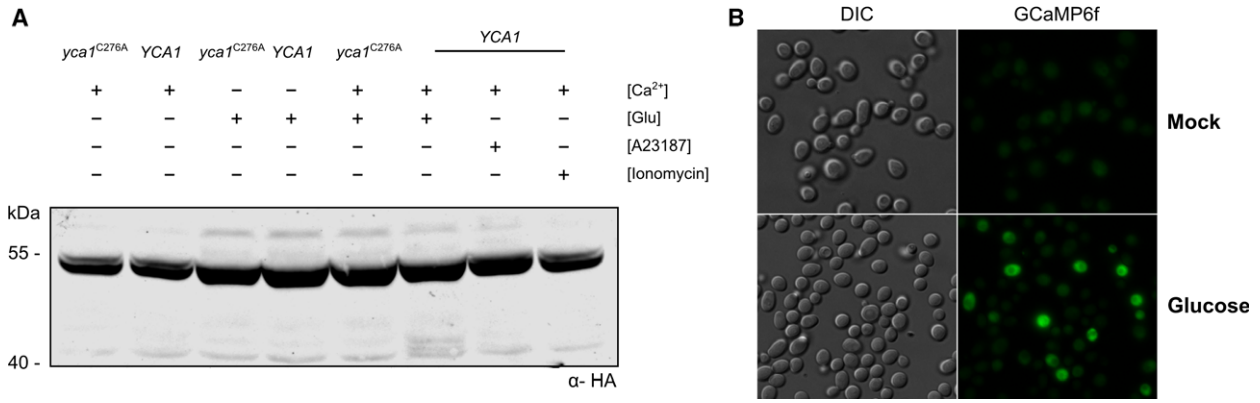

Fig. 7. Ddi1p is cleaved *in vivo* under specific metabolic conditions. (A) Nutrient starved yeast cells expressing HA-tagged versions of Ddi1p at the endogenous locus (HA:Ddi1p) from different metacaspase backgrounds (wild-type *YCA1* and inactive *yca1*^{C276A} mutant) were pre-incubated in the presence (+) or absence (–) of 10 mM calcium for 1 h before the addition of 25 mM glucose (Glu) or calcium ionophores (10 μM A23187 or 1 μM Ionomycin). After 2 h cells were harvested and analyzed by immunoblot with anti-HA antibody. (B) The transient elevation of cytosolic calcium was verified by the increase in fluorescence of the genetically encoded calcium indicator GCaMP6f in mock treated cells (upper panel) or after triggering influx with the addition of 25 mM glucose (lower panel).

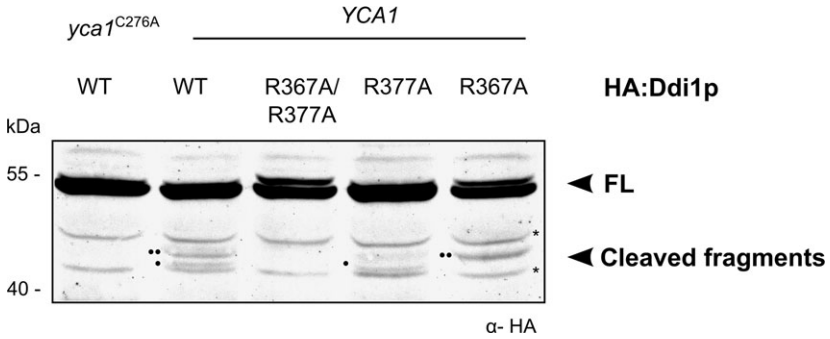

Fig. 8. Ddi1p is cleaved *in vivo* at R367 and R377. Yeast cultures expressing HA:Ddi1p were subjected to glucose mediated transient elevation of cytosolic calcium. HA-Ddi1p full lenght (FL) and its cleavage products were detected by western blot analysis using anti-HA antibodies. Cleaved fragments are depicted with one (cleavage at R367) or two (cleavage at R377) closed circles. Asterisks indicate nonspecific bands that are recognized by the anti-HA antibody.

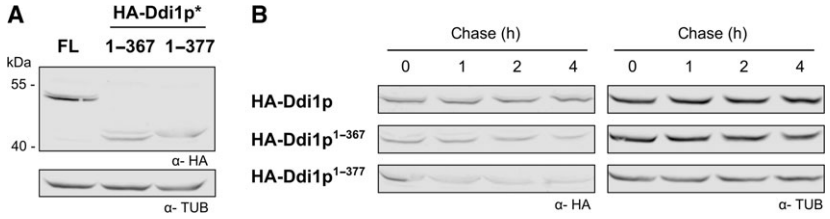

Fig. 9. UBA domain stabilizes Ddi1p. (A) Steady-state levels of HA-tagged Ddi1 variants (FL: full length Ddi1p, 1-367: truncated version at R367, 1-377: truncated version at R377) determined by western blotting with an anti-HA specific antibody. (B) Degradation of HA-tagged Ddi1p variants after blocking translation with 0.5 mg·mL^{-1} cycloheximide. Samples were taken at the indicated time points and probed with anti-HA antibody. α-tubulin is shown as loading control. Bands were detected using an Odyssey laser-scanning system, quantified with Image Studio software and values were fitted to a first-order decay model.

peptide substrate can be processed *in vivo* by Yca1p suggests that the appropriate three dimensional context and surface presentation are important for efficient hydrolysis. The finding that the catalytic efficiencies of trypanosome metacaspases for Ddi1 proteins are 150- to 1000-fold higher than those obtained for each

Table 2. Experimentally identified type I metacaspase auto processing and cleavage sites in protein substrates.

Metacaspase	Cleaved protein	Clevage site sequence	P1 position	Reference
Autoprocessing				
*Tb*MCA2	*Tb*MCA2	FRDA**K**GLHG	55	[53]
		SADV**K**NTAT	268	[53]
Yca1p	Yca1p	MAYN**R**PVYP	72*	[5]
		QEQA**K**AQLS	86*	[5]
		GSIF**K**TVKG	331	[5]
		FKTV**K**GGMG	334	[5]
Substrates				
*Tb*MCA2	EF-Tu	TPIV**R**GSAL	172	[53]
	EF-Tu	GSAL**K**ALEG	177	[53]
	His-*Tb*MCA2	GLVP**R**GSHM	−4	[53]
*Tc*MCA5	*Tc*DDI1	KGQQ**R**GSAR	377	*This work*
*Tb*MCA5	*Tb*DDI1	EEPH**R**GTPF	292	*This work*
	*Tb*DDI1	TAAK**R**STAP	324	*This work*
Yca1p	Ddi1p	ALAP**R**TGMG	367	*This work*
	Ddi1p	TPTG**R**STAG	377	*This work*

*Calcium dependent. Bold letter is used to indicate the site of cleavage.

corresponding peptide substrate strongly supports this hypothesis. These results indicate that metacaspases are extremely selective enzymes possibly requiring extended interactions with the substrate beyond those established within the active site. In this context, the high affinity of *Tc*MCA5 for the *Tc*Ddi1 protein substrate (K_M in the nanomolar range) as well as the low turnover of the enzyme might explain the occurrence of a protein substrate among a set of interactors. Nevertheless, the ability of pull-down assays in identifying protease substrates is limited by the intrinsic transient nature of their interaction and is restricted to a few examples [27,28].

Removal of the C-terminal UBA domain by metacaspase can significantly alter the properties of Ddi1 proteins. This domain is a small motif (≈ 45 residues long) shown to interact with ubiquitin [29,30] that is frequently found in proteins associated with the ubiquitin-proteasome system [31,32]. The expression of Ddi1p protein variants that simulate the loss of the C-terminal UBA domain by Yca1p cleavage at R367 or R377, showed a significant reduction in their steady state abundances as well as stabilities when compared to those of the wild-type full length protein. These results are in agreement with the protein stabilization function assigned to UBA domains [33–35]. Full length Ddi1p contains a 62 residue long disordered region between the RVP and UBA domains [36]. Such an internal unstructured loop is too short to act as a proteasomal initiation region, however, cleavage by Yca1p not only removes the UBA domain but yields a 42 to 52 residue long disordered C-terminus that might be engaged by the proteasome much more efficiently [35]. In addition this internal loop contains a predicted PEST sequence [22] that might further direct Ddi1p to degradation after cleavage. To date all UBA related stability studies have been performed with synthetic and chimeric constructs, thus the proteolytic removal of UBA domains could be considered a novel *in vivo* mechanism as a means to affect turnover of certain proteins.

Although stability loss might determine the ultimate fate of Ddi1p, cleavage by Yca1p can have other more immediate effects. Some Ddi1p functions, such as Ho endonuclease turnover [37] as well as its participation in S-phase checkpoint control [38] require the C-terminal UBA domain. Interestingly, Rad23p, which has partially redundant roles with Ddi1p in cell cycle control [39], was identified as a potential Yca1p modulated protein, although no processing evidence was detected [10]. On the other hand, metacaspase could affect the role of Ddi1p as a secretory repressor since cleavage disrupts the linker region between the RVP and UBA domains (residues 344 to 395), shown to be required for interaction with the exocytic t-SNARE Sso1p [22].

In yeast, Yca1p-mediated Ddi1p cleavage appears to be a tightly regulated event. No processing could be observed during log phase growth or after H_2O_2 treatment, heat shock or extended stationary phase growth (not shown) despite that these stimuli have been associated to metacaspase activation as evidenced by its autoproteolytic cleavage [14,40]. In this work, we have found that *in vivo* Ddi1p processing by Yca1p can be detected after a transient elevation of cytosolic calcium in response to glucose re-addition to carbohydrate starved yeast cells (G-TECC).

In G-TECC two main methodological steps can be distinguished [24]. First, a glucose starvation phase that conduces to a complex reprogramming of yeast metabolism. Among the physiological changes manifested by nutrient deprived cells, the induction of the general stress response and autophagic pathways [41] are events that, noteworthy, also take place in null-*yca1* yeast strains [42]. Moreover, in *Leishmania major*, metacaspase has been linked directly to autophagy as a response to serum deprivation and proposed to act on or upstream of ATG8 [43].

The second methodological step in G-TECC corresponds to the addition of glucose to the cell suspension triggering the influx of extracellular calcium [24]. Successful Ddi1p cleavage by Yca1p relies on supplemented Ca^{2+} ions, however, no processing could be detected when ionophores were used instead of glucose

(Fig. 7A). These results suggest that other stimuli rather than the sole increase in cytosolic Ca^{2+} are required for Yca1p mediated processing of Ddi1p and it is likely that these involve, at least to some extent, glucose signaling pathways. In this sense, considering metacaspase downstream effects, it is remarkable how the increasing evidences hint at a possible association with carbohydrate metabolism. Different proteins, including various enzymes that are involved in glycolytic pathways, have their abundances altered as a consequence of *YCA1* deletion [42,44,45]. Moreover, even in divergent organisms, potential as well as confirmed metacaspase substrates correspond to enzymes that participate in carbohydrate metabolism [16,18–20]. In perspective, these results highlight the possibility that different signaling pathways might lead to cleavage of alternative sets of substrates.

Recently, by means of a proteomics approach, the Ddi1 orthologue of the divergent yeast *Candida albicans* was identified as a potential metacaspase substrate [20]. This variant lacks the C-terminal UBA domain and the disordered region which is a property shared with mammalian isoforms [21]. Remarkably, the putative cleavage site lies at the α-helical domain that links the UbL and RVP domains [36]. This suggests that even though the substrate is conserved the proteolytic event followed divergent evolutionary pathways.

Materials and methods

Expression of recombinant proteins in bacteria

The list of plasmids used for heterologous expression of metacaspases and Ddi1 proteins can be found in Table S2. *Escherichia coli* BL21 Codon Plus (DE3) bacteria transformed with the different constructs were cultured in Luria-Bertani (LB) medium at 37 °C with vigorous shaking (250 r.p.m.) to an OD_{600} of 0.6, and then induced for 3 h at 37 °C with 0.2% w/v arabinose (Sigma-Aldrich, St. Louis, MO, USA). Soluble expression of wild-type Yca1p-GST and *Tb*MCA5-GST as well as inactive mutant derivatives was achieved at 18 °C for 16 h.

For coexpression assays bacteria transformed with pBAD-*Tc*MCA5-3xFLAG or pBAD-*Tc*MCA5(C201A)-3xFLAG were used for the preparation of $CaCl_2$ competent cells and subsequently transformed with pBAD-SC-*Tc*DDI1-GST. Cells were harvested by centrifugation and resuspended in lysis buffer (50 mM TrisHCl, 150 mM NaCl, 0.2 $mg{\cdot}mL^{-1}$ lysozyme, 0.1% Triton X-100, 1 mM phenylmethylsulfonyl fluoride (PMSF) pH 7.6) and sonicated. Samples were centrifuged for 30 min at 23 000 × ***g*** to obtain the bacterial crude extracts. Soluble fractions were analyzed by western blot.

To study *Tc*MCA5/*Tc*DDI1 interaction, clarified extracts supplemented or not with 10 mM DTT (Promega, Fitchburg, WI, USA) and 100 μM $CaCl_2$ were incubated with glutathione-agarose resin (GE Healthcare, Chicago, IL, USA) equilibrated in TBS (50 mM TrisHCl pH 7.6, 150 mM NaCl) for 30 min at 4 °C. Resin was washed ten times with TBS. The bound proteins were eluted with 50 mM TrisHCl pH 8.8 containing 20 mM reduced glutathione. Samples were analyzed by western blot.

For recombinant protein purification bacteria were harvested by centrifugation, resuspended in lysis buffer, and sonicated when necessary. Samples were centrifuged at 23 000 × ***g*** for 30 min at 4 °C to obtain the bacterial crude extract. DTT was added to a final concentration of 1 mM. The recombinant proteins were purified using a glutathione-agarose resin (GE Healthcare) equilibrated with TBS buffer. The columns were washed with 20 column volumes of TBS and the samples were eluted with 50 mM TrisHCl pH 8.8 containing 20 mM reduced glutathione.

In vitro metacaspase-mediated Ddi1 cleavage assay

Purified Ddi1 recombinant proteins (25 μg) were mixed with purified recombinant metacaspases or their corresponding active site mutants (2.5 μg) in 200 μL of 50 mM HEPES pH 7.2 containing 100 μM $CaCl_2$, 10 mM DTT, and 10% glycerol. The protein mixtures were incubated at 37 °C for 16 h and reactions were stopped by the addition of Laemmli sample buffer and 5 min of boiling. Fifteen microliters of each sample were analyzed by western blot.

Kinetic rate constants were studied as described in [46]. Briefly, metacaspases were incubated with various concentrations of Ddi1 proteins and cleavage was subsequently assessed by 12.5% SDS/PAGE, followed by western blot. Blots were scanned on an Odyssey infrared scanner (LI-COR Biosciences, Lincoln, NE, USA) and the fluorescent signal of full-length Ddi1 proteins and the cleaved products were used to determine the processing rates. The obtained values were fitted to a hyperbolic 2-parameter, single rectangular Michaelis-Menten function ($v = V_{max}\,[S]/K_M + [S]$) using GraphPad Prism software (GraphPad Software Inc, La Jolla, CA, USA). Metacaspase concentration was determined by titration with the irreversible inhibitor z-VRPR-FMK as described below.

Metacaspase enzymatic assay using FRET peptides

Cleavage site sequences identified in Ddi1 orthologues were synthesized by GenScript (Piscataway, NJ, USA) as highly sensitive FRET substrates, bearing an ortho-aminobenzoyl (Abz) fluorescent group and an N-(2,4-dinitrophenyl)-ethylenediamine (Dnp) quenching group, as the donor/acceptor pair. FRET substrates were dissolved in DMSO

(Sigma-Aldrich) and the concentration was obtained by colorimetric determination of the K(Dnp) group (ε = 17 300 $M^{-1} \cdot cm^{-1}$ at 365 nm). To determine metacaspase activity, each substrate (final concentration 10 μM to avoid inner filtering effect) was incubated with Yca1p-GST (final concentration 8.24×10^{-9} M), *Tc*MCA5-GST (final concentration 9.9×10^{-7} M) and *Tb*MCA5-GST (final concentration 8.23×10^{-8} M) in 200 μL of 50 mM HEPES pH 7.5 containing 10 mM DTT and optimized concentrations of $CaCl_2$ (Yca1p-GST: 800 μM; *Tb*MCA5-GST and *Tc*MCA5-GST: 100 μM). The increase in fluorescence resulting from peptide-cleavage was continuously monitored (excitation: 320 nm; emission 420 nm; sensitivity: 750 volts) over 1800 s at 30 °C with an Aminco Bowman Series 2 spectrofluorometer (Thermo Spectronic, Madison, WI, USA). In the case of Abz-PTGRSTAK(Dnp), which resulted resistant to metacaspase hydrolysis, substrate functionality was positively confirmed by cruzipain hydrolysis under described conditions [47].

Catalytic efficiency (k_{cat}/K_M) for the hydrolysis of FRET peptides by metacaspases were evaluated at low substrate concentrations. Metacaspase activity was assayed at 30 °C for decreasing substrate concentrations (ranging from 10 to 0625 μM) in the same buffers described above (supplemented with 0.01% Triton X-100). Assay was performed in a solid black 384-well plate (final reaction volume ~ 50 μL) and fluorescence was monitored continuously with a FilterMax F5 Multi-Mode Microplate Reader (Molecular Devices, Sunnyvale, CA, USA) using standard 320 nm excitation and 430 nm emission filter set. Active site concentration of *T. cruzi*, *T. brucei* and yeast metacaspases was determined by titration using the irreversible inhibitor Z-VRPR-FMK (GenScript) as described in [48]. For k_{cat}/K_M estimation, only data in the linear portion of the Michaelis-Menten plot (first-order conditions: $[S_0] << K_M$) were considered.

Electrophoresis and immunoblotting

Proteins were separated by SDS/PAGE (10 or 12.5% acrylamide) and transferred to a nitrocellulose Hybond ECL membrane (GE Healthcare) for probing with anti-FLAG M2 mouse monoclonal antibody (Sigma-Aldrich) diluted 1 : 2500 or anti-GST (clone 2H3D10) mouse monoclonal antibody diluted 1 : 2000 (Sigma-Aldrich). Anti-HA High Affinity (clone 3F10) was purchased from Roche (Basel, Switzerland). Monoclonal anti α-tubulin 1 : 5000 clone B-5-1-2 (Sigma-Aldrich) was used as loading control. Horseradish peroxidase-conjugated goat anti-mouse secondary antibody (Sigma-Aldrich) diluted 1 : 5000 was detected by chemiluminescence using SuperSignal West Pico Chemiluminescent Substrate (Pierce, Rockford, IL, USA). Alternatively, blots were probed with Alexa Fluor® 790 AffiniPure Goat Anti-Rat IgG (H + L) or Alexa Fluor® 680 AffiniPure Goat Anti-Mouse IgG (H + L) secondary antibodies (Jackson Immunoresearch Laboratories, West Grove, PA, USA), signal intensities were detected using an Odyssey laser-scanning system and quantified with Image Studio software (LI-COR Biosciences). Prestained Protein Molecular Weight markers used were from Pierce.

N-terminal sequencing

For N-terminal sequencing, proteins separated by SDS/PAGE were transferred to a PVDF membrane (Merck Millipore, Burlington, MA, USA). Ddi1 digested fragments were excised from the membrane and sent to The Protein Facility of the Iowa State University for Edman N-terminal sequencing.

Yeast strains and plasmids

Saccharomyces cerevisiae wild-type background strain BY4742 (MATα; *his3*Δ1; *leu2*Δ0; *lys2*Δ0; *ura3*Δ0) and *YCA1* disruption strain Y12453 (BY4742; *YOR197w*::*kan*MX4) were obtained from the European *Saccharomyces cerevisiae* archive for functional analysis (EUROSCARF, Oberursel, Germany). For the list of strains that express $yca1^{C276A}$ inactive mutant and different N-terminal HA tagged variants of Ddi1p as well as the plasmids used in their generation see Table S3. For the expression of GCaMP6f, yeasts were transformed with PvuII linearized pRS306K-GPD1p-ADH1t-a-GCaMP6f [49] (kindly provided by Dr. Pablo S. Aguilar, Instituto de Investigaciones Biotecnológicas, Universidad de San Martin, San Martin, Argentina).

Yeast culture and media

For routine culture of yeasts YPDA medium (1% w/v yeast extract (BD, Franklin Lakes, NJ, USA), 2% w/v tryptone (BD), 2% w/v glucose (Sigma-Aldrich), 0.02% w/v adenine (Sigma-Aldrich) was used. For selection of cells transformed with *kan*MX bearing genetic constructs the medium was supplemented with 200 $\mu g \cdot mL^{-1}$ of G418 (Thermo Fisher, Waltham, MA, USA). For selective growth of auxotrophic strains and oxidative stress experiments SCD medium (0.67% w/v yeast nitrogen base with ammonium sulfate (BD), 0.192% w/v yeast synthetic drop-out medium with or without uracil (Sigma-Aldrich), 2% w/v glucose (Sigma-Aldrich) was used instead. Counter selection of *URA3* was performed on SCD media supplemented with 1 $mg \cdot mL^{-1}$ of 5-fluoroorotic acid (5-FOA) (Zymo Research, Irvine, CA, USA). Solid media was obtained by the addition of 2% w/v bacto-agar (BD). Yeasts were cultured at 30 °C with vigorous shaking (250 r.p.m.).

Yeast extracts for western blots

The mild alkali treatment protocol was employed [50]. Briefly cells were harvested by centrifugation at 5000 × ***g*** for 30 min at 4 °C and resuspended with water to a density

of OD_{600} 25 per mL, further diluted with the addition of one volume of 200 mM NaOH and incubated for 10 min on ice. Afterwards cells were centrifuged, resuspended in water to a density of OD_{600} 100 per mL, diluted by addition of a volume of 2 × concentrate Laemmli sample buffer and boiled for 5 min. An equivalent of OD_{600} 1 was loaded per lane and resolved by SDS/PAGE electrophoresis.

Glucose mediated transient elevation of cytosolic calcium

Glucose starvation and glucose readdition were carried out essentially as described in [24]. Briefly, exponentially growing cells in SCD medium containing 2% glucose were harvested, washed and resuspended in SCD medium containing 0.02% glucose to a final density of $1x10^6$ cells per mL. After incubation for 24 h at 28 °C, starved cultures were harvested by centrifugation, washed once with 0.1 M 2-(N-morpholino)ethanesulfonic acid adjusted with 1 M Tris (pH 10.8) to pH 6.5 (MES/Tris buffer). Cells were resuspended in the same buffer, incubated for 2 h at 28 °C, and then $CaCl_2$ was supplemented to 10 mM final concentration. Transient elevation of cytosolic calcium was triggered by the addition of glucose to 25 mM final concentration. For western blot analysis cells were lysed and an equivalent of OD_{600} 1 was loaded per lane. Alternatively, starved cells were allowed to bind to poly-L-lysine coated coverslips in $CaCl_2$ supplemented MES/Tris buffer and GCaMP6f fluorescence was monitored with an Eclipse 80i microscope (Nikon, Shinagawa, Japan) after triggering calcium influx by the addition of 25 mM glucose.

Cycloheximide chase analysis

Degradation kinetics of Ddi1p were studied as described in [51]. Briefly, overnight grown yeast cultures were diluted to an OD_{600} value of 0.2 in fresh YPDA medium, and incubated at 30 °C with vigorous shaking (250 r.p.m.) until the cells reached midlogarithmic growth phase (an OD_{600} between 0.8 and 1.2). To terminate protein synthesis, cycloheximide was added to 500 $\mu g \cdot mL^{-1}$ final concentration. Cells were collected at specific time points, lysed and separated by SDS/PAGE followed by western blot analysis. Bands were quantified with Image Studio software and values were fitted to a first-order decay model [52].

Acknowledgments

This study was supported by PICT 2013-1498 from the Agencia Nacional de Promoción Científica y Tecnológica (ANPCyT, MinCyT), Argentina to VEA; PICT 2014-1410 from ANPCyT, MinCyT, Argentina to JJC, PICT 2014-3029 from ANPCyT, MinCyT, Argentina to LAB and Fundación Bunge y Born to LAB. LAB, GTN, JJC and VEA are members of the research career of the Argentinean National Research Council (CONICET). We are grateful to Dr. Pablo S. Aguilar, Instituto de Investigaciones Biotecnológicas, San Martin, Buenos Aires, Argentina for kindly providing vector pRS306K-GPD1p-ADH1t-a-GCaMP6f and technical assistance.

Conflict of interest

The authors declare no conflict of interest.

Author contributions

LAB and GTN conducted most of the experiments, analyzed the results, and prepared the Figures. ESS conducted experiments on enzymatic assay using FRET peptides. LAB, GTN, ESS, JJC, and VEA contributed with critical discussions of all sections and produced the final manuscript. All authors reviewed the manuscript.

References

1 Uren AG, O'Rourke K, Aravind LA, Pisabarro MT, Seshagiri S, Koonin EV & Dixit VM (2000) Identification of paracaspases and metacaspases: two ancient families of caspase-like proteins, one of which plays a key role in MALT lymphoma. *Mol Cell* **6**, 961–967.

2 Hachmann J & Salvesen GS (2016) The Paracaspase MALT1. *Biochimie* **122**, 324–338.

3 Fagundes D, Bohn B, Cabreira C, Leipelt F, Dias N, Bodanese-Zanettini MH & Cagliari A (2015) Caspases in plants: metacaspase gene family in plant stress responses. *Funct Integr Genomics* **15**, 639–649.

4 McLuskey K, Rudolf J, Proto WR, Isaacs NW, Coombs GH, Moss CX & Mottram JC (2012) Crystal structure of a Trypanosoma brucei metacaspase. *Proc Natl Acad Sci USA* **109**, 7469–7474.

5 Wong AH, Yan C & Shi Y (2012) Crystal structure of the yeast metacaspase Yca1. *J Biol Chem* **287**, 29251–29259.

6 Suarez MF, Filonova LH, Smertenko A, Savenkov EI, Clapham DH, von Arnold S, Zhivotovsky B & Bozhkov PV (2004) Metacaspase-dependent programmed cell death is essential for plant embryogenesis. *Curr Biol* **14**, R339–R340.

7 Bozhkov PV, Suarez MF, Filonova LH, Daniel G, Zamyatnin AA Jr, Rodriguez-Nieto S, Zhivotovsky B & Smertenko A (2005) Cysteine protease mcII-Pa executes programmed cell death during plant embryogenesis. *Proc Natl Acad Sci USA* **102**, 14463–14468.

8 Coll NS, Vercammen D, Smidler A, Clover C, Van Breusegem F, Dangl JL & Epple P (2010) Arabidopsis

type I metacaspases control cell death. *Science* **330**, 1393–1397.
9 Wrzaczek M, Vainonen JP, Stael S, Tsiatsiani L, Help-Rinta-Rahko H, Gauthier A, Kaufholdt D, Bollhoner B, Lamminmaki A, Staes A *et al.* (2015) GRIM REAPER peptide binds to receptor kinase PRK5 to trigger cell death in Arabidopsis. *EMBO J* **34**, 55–66.
10 Lee RE, Puente LG, Kaern M & Megeney LA (2008) A non-death role of the yeast metacaspase: Yca1p alters cell cycle dynamics. *PLoS ONE* **3**, e2956.
11 Helms MJ, Ambit A, Appleton P, Tetley L, Coombs GH & Mottram JC (2006) Bloodstream form Trypanosoma brucei depend upon multiple metacaspases associated with RAB11-positive endosomes. *J Cell Sci* **119**, 1105–1117.
12 Ambit A, Fasel N, Coombs GH & Mottram JC (2008) An essential role for the Leishmania major metacaspase in cell cycle progression. *Cell Death Differ* **15**, 113–122.
13 Laverriere M, Cazzulo JJ & Alvarez VE (2012) Antagonic activities of Trypanosoma cruzi metacaspases affect the balance between cell proliferation, death and differentiation. *Cell Death Differ* **19**, 1358–1369.
14 Hill SM, Hao X, Liu B & Nystrom T (2014) Life-span extension by a metacaspase in the yeast Saccharomyces cerevisiae. *Science* **344**, 1389–1392.
15 Sundstrom JF, Vaculova A, Smertenko AP, Savenkov EI, Golovko A, Minina E, Tiwari BS, Rodriguez-Nieto S, Zamyatnin AA Jr, Valineva T *et al.* (2009) Tudor staphylococcal nuclease is an evolutionarily conserved component of the programmed cell death degradome. *Nat Cell Biol* **11**, 1347–1354.
16 Silva A, Almeida B, Sampaio-Marques B, Reis MI, Ohlmeier S, Rodrigues F, Vale A & Ludovico P (2011) Glyceraldehyde-3-phosphate dehydrogenase (GAPDH) is a specific substrate of yeast metacaspase. *Biochim Biophys Acta* **1813**, 2044–2049.
17 Strobel I & Osiewacz HD (2013) Poly(ADP-ribose) polymerase is a substrate recognized by two metacaspases of Podospora anserina. *Eukaryot Cell* **12**, 900–912.
18 Tsiatsiani L, Timmerman E, De Bock PJ, Vercammen D, Stael S, van de Cotte B, Staes A, Goethals M, Beunens T, Van Damme P *et al.* (2013) The Arabidopsis metacaspase9 degradome. *Plant Cell* **25**, 2831–2847.
19 Leger T, Garcia C, Ounissi M, Lelandais G & Camadro JM (2015) The metacaspase (Mca1p) has a dual role in farnesol-induced apoptosis in Candida albicans. *Mol Cell Proteomics* **14**, 93–108.
20 Leger T, Garcia C & Camadro JM (2016) The metacaspase (Mca1p) restricts o-glycosylation during farnesol-induced apoptosis in candida albicans. *Mol Cell Proteomics* **15**, 2308–2323.
21 Nowicka U, Zhang D, Walker O, Krutauz D, Castaneda CA, Chaturvedi A, Chen TY, Reis N, Glickman MH & Fushman D (2015) DNA-damage-inducible 1 protein (Ddi1) contains an uncharacteristic ubiquitin-like domain that binds ubiquitin. *Structure* **23**, 542–557.
22 Gabriely G, Kama R, Gelin-Licht R & Gerst JE (2008) Different domains of the UBL-UBA ubiquitin receptor, Ddi1/Vsm1, are involved in its multiple cellular roles. *Mol Biol Cell* **19**, 3625–3637.
23 Nakajima-Shimada J, Iida H, Tsuji FI & Anraku Y (1991) Monitoring of intracellular calcium in Saccharomyces cerevisiae with an apoaequorin cDNA expression system. *Proc Natl Acad Sci USA* **88**, 6878–6882.
24 Kaibuchi K, Miyajima A, Arai K & Matsumoto K (1986) Possible involvement of RAS-encoded proteins in glucose-induced inositolphospholipid turnover in Saccharomyces cerevisiae. *Proc Natl Acad Sci USA* **83**, 8172–8176.
25 Hachmann J, Snipas SJ, van Raam BJ, Cancino EM, Houlihan EJ, Poreba M, Kasperkiewicz P, Drag M & Salvesen GS (2012) Mechanism and specificity of the human paracaspase MALT1. *Biochem J.* **443**, 287–295.
26 Machado MF, Marcondes MF, Juliano MA, McLuskey K, Mottram JC, Moss CX, Juliano L & Oliveira V (2013) Substrate specificity and the effect of calcium on Trypanosoma brucei metacaspase 2. *FEBS J* **280**, 2608–2621.
27 Lopez-Otin C & Overall CM (2002) Protease degradomics: a new challenge for proteomics. *Nat Rev Mol Cell Biol* **3**, 509–519.
28 Jager S, Cimermancic P, Gulbahce N, Johnson JR, McGovern KE, Clarke SC, Shales M, Mercenne G, Pache L, Li K *et al.* (2011) Global landscape of HIV-human protein complexes. *Nature* **481**, 365–370.
29 Bertolaet BL, Clarke DJ, Wolff M, Watson MH, Henze M, Divita G & Reed SI (2001) UBA domains of DNA damage-inducible proteins interact with ubiquitin. *Nat Struct Biol* **8**, 417–422.
30 Wilkinson CR, Seeger M, Hartmann-Petersen R, Stone M, Wallace M, Semple C & Gordon C (2001) Proteins containing the UBA domain are able to bind to multi-ubiquitin chains. *Nat Cell Biol* **3**, 939–943.
31 Hofmann K & Bucher P (1996) The UBA domain: a sequence motif present in multiple enzyme classes of the ubiquitination pathway. *Trends Biochem Sci* **21**, 172–173.
32 Su V & Lau AF (2009) Ubiquitin-like and ubiquitin-associated domain proteins: significance in proteasomal degradation. *Cell Mol Life Sci* **66**, 2819–2833.
33 Heessen S, Masucci MG & Dantuma NP (2005) The UBA2 domain functions as an intrinsic stabilization signal that protects Rad23 from proteasomal degradation. *Mol Cell* **18**, 225–235.

34 Heinen C, Acs K, Hoogstraten D & Dantuma NP (2011) C-terminal UBA domains protect ubiquitin receptors by preventing initiation of protein degradation. *Nat Commun* **2**, 191.
35 Fishbain S, Prakash S, Herrig A, Elsasser S & Matouschek A (2011) Rad23 escapes degradation because it lacks a proteasome initiation region. *Nat Commun* **2**, 192.
36 Trempe JF, Saskova KG, Siva M, Ratcliffe CD, Veverka V, Hoegl A, Menade M, Feng X, Shenker S, Svoboda M *et al.* (2016) Structural studies of the yeast DNA damage-inducible protein Ddi1 reveal domain architecture of this eukaryotic protein family. *Sci Rep* **6**, 33671.
37 Kaplun L, Tzirkin R, Bakhrat A, Shabek N, Ivantsiv Y & Raveh D (2005) The DNA damage-inducible UbL-UbA protein Ddi1 participates in Mec1-mediated degradation of Ho endonuclease. *Mol Cell Biol* **25**, 5355–5362.
38 Clarke DJ, Mondesert G, Segal M, Bertolaet BL, Jensen S, Wolff M, Henze M & Reed SI (2001) Dosage suppressors of pds1 implicate ubiquitin-associated domains in checkpoint control. *Mol Cell Biol* **21**, 1997–2007.
39 Diaz-Martinez LA, Kang Y, Walters KJ & Clarke DJ (2006) Yeast UBL-UBA proteins have partially redundant functions in cell cycle control. *Cell Div* **1**, 28.
40 Madeo F, Herker E, Maldener C, Wissing S, Lachelt S, Herlan M, Fehr M, Lauber K, Sigrist SJ, Wesselborg S *et al.* (2002) A caspase-related protease regulates apoptosis in yeast. *Mol Cell* **9**, 911–917.
41 Dechant R & Peter M (2008) Nutrient signals driving cell growth. *Curr Opin Cell Biol* **20**, 678–687.
42 Lee RE, Brunette S, Puente LG & Megeney LA (2010) Metacaspase Yca1 is required for clearance of insoluble protein aggregates. *Proc Natl Acad Sci USA* **107**, 13348–13353.
43 Casanova M, Gonzalez IJ, Sprissler C, Zalila H, Dacher M, Basmaciyan L, Spath GF, Azas N & Fasel N (2015) Implication of different domains of the Leishmania major metacaspase in cell death and autophagy. *Cell Death Dis* **6**, e1933.
44 Zdralevic M, Longo V, Guaragnella N, Giannattasio S, Timperio AM & Zolla L (2015) Differential proteome-metabolome profiling of YCA1-knock-out and wild type cells reveals novel metabolic pathways and cellular processes dependent on the yeast metacaspase. *Mol BioSyst* **11**, 1573–1583.
45 Longo V, Zdralevic M, Guaragnella N, Giannattasio S, Zolla L & Timperio AM (2015) Proteome and metabolome profiling of wild-type and YCA1-knock-out yeast cells during acetic acid-induced programmed cell death. *J Proteomics* **128**, 173–188.
46 Reverter D & Lima CD (2009) Preparation of SUMO proteases and kinetic analysis using endogenous substrates. *Methods Mol Biol* **497**, 225–239.
47 Alvarez VE, Niemirowicz GT & Cazzulo JJ (2012) The peptidases of Trypanosoma cruzi: digestive enzymes, virulence factors, and mediators of autophagy and programmed cell death. *Biochim Biophys Acta* **1824**, 195–206.
48 Stennicke HR & Salvesen GS (1999) Caspases: preparation and characterization. *Methods* **17**, 313–319.
49 Carbo N, Tarkowski N, Ipina EP, Dawson SP & Aguilar PS (2017) Sexual pheromone modulates the frequency of cytosolic Ca2 + bursts in Saccharomyces cerevisiae. *Mol Biol Cell* **28**, 501–510.
50 Kushnirov VV (2000) Rapid and reliable protein extraction from yeast. *Yeast* **16**, 857–860.
51 Buchanan BW, Lloyd ME, Engle SM & Rubenstein EM (2016) Cycloheximide chase analysis of protein degradation in saccharomyces cerevisiae. *J Vis Exp* **110**, 53975.
52 Belle A, Tanay A, Bitincka L, Shamir R & O'Shea EK (2006) Quantification of protein half-lives in the budding yeast proteome. *Proc Natl Acad Sci USA* **103**, 13004–13009.
53 Moss CX, Westrop GD, Juliano L, Coombs GH & Mottram JC (2007) Metacaspase 2 of Trypanosoma brucei is a calcium-dependent cysteine peptidase active without processing. *FEBS Lett* **581**, 5635–5639.

Supporting information

Additional Supporting Information may be found online in the supporting information tab for this article:

Table S1. List of putative metacaspase interacting proteins.

Table S2. Plasmids for the heterologous expression of metacaspases and interactors in *Escherichia coli*.

Table S3. Yeast strains and plasmids used in their obtention.